LIMNOLOGY and OCEANOGRAPHY

ASLO

Limnol. Oceanogr. 71, 2026, e70315

doi: 10.1002/lno.70315

RESEARCH ARTICLE

Microbial nitrogen removal and recycling in the redox transition zone of a meromictic lake and its coupling to sulfur cycling

Jana Tischer,[1*] **Moritz F. Lehmann**,[1] **Guangyi Su**,[1] **Fabio Lepori**,[2,3] **Jakob Zopfi**[1*]

[1]Department of Environmental Sciences, University of Basel, Basel, Switzerland; [2]Department for Environment, Constructions and Design, University of Applied Sciences and Arts of Southern Switzerland, Canobbio, Switzerland; [3]Directorate General of Environment, Canton of Vaud, Lausanne, Switzerland

Abstract

Organotrophic denitrification is an important nitrogen (N) removal process in lakes, but alternative N reduction processes such as lithotrophic sulfur (S)-oxidizing denitrification may be greatly underappreciated. We studied the redox transition zone (RTZ) in the meromictic water column of the North Basin of Lake Lugano (Switzerland) to characterize N transformation pathways coupled to the S and carbon (C) cycles. Incubations with ^{15}N-labeled and unlabeled nitrate (NO_3^-) revealed low denitrification rates and a general limitation of organic electron donors. The most accessible fractions of exported primary production biomass may have been largely consumed in the oxic water column during sedimentation and did not reach the RTZ at ~ 100 m depth. Conversely, sulfide (H_2S) and methane (CH_4), major end products of anaerobic degradation of the more recalcitrant organic carbon fractions in the sediment, represent a continuous source of energy to the RTZ, fostering the establishment of a community of S- and CH_4-dependent NO_3^- reducers, dominated by *Sulfuritalea* and *Candidatus* Methylomirabilis over several years of observation. Anoxic incubation experiments with H_2S amendments revealed a strong stimulation of dissimilatory NO_3^- reduction to ammonium (NH_4^+) (DNRA), but not denitrification. High relative abundances of the archaeal NH_4^+ oxidizer *Candidatus* Nitrosopumilus and bacterial nitrifiers indicate intense NO_3^- regeneration by nitrification in the upper RTZ. The potential interaction between nitrification and S-driven DNRA is unclear. However, their co-occurrence suggests that, at least under conditions of carbon limitation, N recycling between the NO_3^- and ammonium pools predominates over N removal via complete denitrification.

Due to the widespread use of fertilizers in agriculture and wastewater release, large amounts of reactive (i.e., fixed) nitrogen (N) have entered and altered natural ecosystems (Gruber and Galloway 2008). It is estimated that up to 75% of the anthropogenic N introduced into inland waters are removed along the freshwater/seawater continuum before reaching coastal marine ecosystems. In this regard, lakes serve as efficient N sinks, playing a particularly important role in mitigating anthropogenic nutrient loads (Howarth et al. 1996). Canonical organotrophic denitrification, the microbial reduction of nitrate (NO_3^-) to dinitrogen gas (N_2) with organic compounds as substrate, is considered to be the most important N removal process (Seitzinger 1988). However, there is increasing evidence for alternative substrates such as methane (CH_4) (Raghoebarsing et al. 2006) and inorganic electron donors like reduced sulfur (S) compounds (Hulth et al. 2005; Burgin and Hamilton 2007). Anaerobic ammonium (NH_4^+) oxidation to N_2 (anammox) and the dissimilatory nitrate reduction to ammonium (DNRA) represent additional N turnover processes in lakes (Schubert et al. 2006; Roland et al. 2018). Yet, the relative contributions of these major N transformations to N cycling, their different trophic modes (i.e., organotrophic vs. lithotrophic), and the responsible microbial actors in lakes are not well understood. This is particularly important for lacustrine N budgets: in contrast to denitrification and anammox, DNRA promotes N recycling rather than fixed-N removal.

*Correspondence: jana.tischer@unibas.ch; jakob.zopfi@unibas.ch

Associate editor: Werner Eckert

Denitrification and DNRA share the initial reduction step from NO_3^- to NO_2^- and can both be carried out by organotrophic or lithotrophic microorganisms (Pandey et al. 2020). DNRA has been found to dominate in experimental systems and natural environments with NO_3^--limiting conditions, such as lake sediments. In contrast, denitrification tends to prevail in high-NO_3^- environments (Kelso et al. 1997; Strohm et al. 2007; Dong et al. 2011). Also, the type and availability of alternative inorganic substrates may affect the mode of NO_3^- reduction (Brunet and Garcia-Gil 1996; Cojean et al. 2020). Organotrophic N reduction is performed by ubiquitous facultative or strict anaerobic microorganisms, including many Proteobacteria, Firmicutes, and Actinobacteria (Shapleigh 2013; Pandey et al. 2020). Moreover, obligate and facultative chemolithotrophic bacteria (e.g., representatives of the *Rhodocyclaceae*, *Sulfurimonadaceae*, or *Hydrogenophilaceae*) can couple the oxidation of sulfide (H_2S), elemental sulfur (S^0), or thiosulfate ($S_2O_3^{2-}$) with the reduction of NO_3^- to NO_2^-, and from there to N_2 or to NH_4^+ (Zumft 1997; Shao et al. 2010; Pandey et al. 2020). Only a few specialized microorganisms are known (e.g., *Candidatus* Methylomirabilis) that oxidize CH_4 anaerobically via NO_3^- or NO_2^- reduction to N_2 (Raghoebarsing et al. 2006; Yao et al. 2024).

The absolute and relative importance of these different N-turnover modes in the natural environment can be highly variable. In lacustrine water columns, reported N-transformation rates vary by several orders of magnitude (i.e., between < 50 nmol N L^{-1} d^{-1} and > 10 μmol N L^{-1} d^{-1}; Supporting Information Table S1). Alternative modes of suboxic N reaction were shown to contribute substantially to total N_2 production (sometimes even exceeding rates of canonical organotrophic denitrification), such as S-dependent denitrification in Wintergreen Lake (Burgin et al. 2012), CH_4-dependent denitrification in several Indian reservoirs (Naqvi et al. 2018), or anammox in Lake Tanganyika (Schubert et al. 2006). Studies that concurrently investigated the rates of denitrification, DNRA, and anammox within the same lake water column are rare. Lake Kivu is an exception, with all three processes confirmed to co-occur there (Roland et al. 2018). These processes, which occur in anoxic lake water bodies and redox transition zones (RTZs), are not unique to meromictic lakes; they may also arise seasonally in eutrophic lakes when thermal stratification leads to temporary hypolimnetic anoxia and sulfide accumulation.

The south-Aalpine Lake Lugano, comprising the weakly connected~~hydrologically separated~~ South Basin (93 m depth) and the deep, narrow North Basin (288 m depth), has been impacted by eutrophication. Phosphorous (P) and N inputs from municipal wastewater led to biogenic meromixis in the North Basin from ~ 1960 onward (Barbieri and Mosello 1992; Lepori et al. 2018; Studer et al. 2024). This meromixis was only interrupted by two mixing events in 2005 and 2006, when cold and windy winters caused complete overturning (Holzner et al. 2009; Lehmann et al. 2015). Wenk et al. (2013, 2014) investigated the modes of N loss in the water column of the North Basin and reported that canonical organotrophic denitrification plays only a minor role as N sink in summer and autumn. Instead, S-driven chemolithotrophic denitrification, and to a much lesser extent anammox, were proposed as the main N-removing processes in the North Basin's RTZ. However, the conditions that promote fixed-N elimination via lithotrophic rather than organotrophic N_2 production—including seasonal fluctuations in organic carbon (C_{org}) export or substrate availability—remained largely unresolved. Furthermore, the extent of N recycling within the RTZ remains uncertain as DNRA in the water column has not been determined to date.

Here we combine ^{15}N isotope-label incubation experiments with multi-year 16S rRNA gene amplicon sequence data to (i) investigate the controls on, and significance of, microbial fixed N removal vs. retention within the RTZ in the meromictic Lake Lugano North Basin; and to (ii) identify key S-oxidizing NO_3^- reducers, as well as other N- and S-transforming microorganisms involved. We examine whether the previously proposed predominance of S-driven denitrification in the RTZ (Wenk et al. 2013) is a permanent or a seasonal feature.

Material and methods

Study site, in situ profiling, and sample collection

We studied the water column of Lake Lugano's North Basin (271 m above sea level) at the deepest spot (46°00′37.7″N, 9°01′14.9″E) in April, June, and October 2015, March, September, and November 2016, February and October 2017, and April 2018. A conductivity, temperature, depth (CTD) probe (Idronaut Ocean Seven 316Plus) was used to determine oxygen (O_2) concentrations, temperature, and conductivity. From July 2016 onward, we measured chlorophyll *a* (Chl *a*) using a TriLux fluorometer attached to the CTD. We used the CTD data to calculate the static stability of the water column (Supporting Information Appendix 1). Monthly primary production and NO_3^- concentration data were obtained through a monitoring program conducted by the University of Applied Sciences and Arts of Southern Switzerland (www.cipais.org).

In this study, the upper RTZ boundary is set at the depth where O_2 falls below 5 μM, and its lower boundary at the depth where oxygen-sensitive reduced chemical compounds like Fe^{2+} or H_2S rise above background levels. Samples were collected across the RTZ starting at around 80 m depth to a maximum depth of 155–165 m using 5 L Niskin bottles. Sample water was filled into sterile 1 L plastic or borosilicate bottles for DNA analysis and into 1 L borosilicate bottles for enrichment cultures, each without leaving headspace. Water samples were kept cold and in the dark until further processing. For DNA analysis of all water samples, a volume of ~ 1.1–1.2 L was filtered through 0.2 μm polycarbonate

membrane filters (Cyclopore, Whatman), without prefilter, within 24 h of sample collection. For ^{15}N-label incubations, water from the Niskin bottle was filled directly into sterile 160 mL serum vials (bubble-free with ~1–2 volumes overflow), and the vials were closed with gray rubber stoppers (VWR), which had been boiled in deionized water for ≥ 30 min and stored under helium (He) atmosphere until usage. The bottles were kept cold and in the dark until the incubation experiments were started in the home laboratory within 10 h after sampling. From each depth, additional samples were collected and prepared for various chemical analyses.

Chemical analyses

Nitrogen species

Water samples for the analysis of dissolved inorganic N concentrations were filtered (0.45 μm pore size) right after collection. NH_4^+ concentrations were determined using the colorimetric indophenol reaction (Hansen and Koroleff 1999) (detection limit ~ 1 μM, 5%–10% measurement uncertainty), and NO_2^- using sulfanilamide and N-(1-Naphthyl)ethylenediamine (Hansen and Koroleff 1999) (detection limit ~ 0.05 μM, 0.5%–2% measurement uncertainty). The sum of NO_2^- and NO_3^- (NO_x) was determined using a NO_x analyzer (Antek Model 745) involving the reduction of NO_x in a hot acidic vanadium(III) choride (VCl_3) solution to nitric oxide (NO) gas, and subsequent chemiluminescence detection (Braman and Hendrix 1989) (detection limit ~ 1 μM, 1%–3% measurement uncertainty). We determined NO_3^- concentrations by subtracting NO_2^- from NO_x concentrations.

Iron

Aliquots of unfiltered and filtered (0.2 μm) water samples were fixed with ~ 150 mM (final concentration) nitric acid (HNO_3) for the analysis of total and dissolved iron concentrations, respectively. Concentrations were quantified by inductively coupled plasma optical emission spectrometry (Agilent Technologies) with a detection limit of ~ 1.8 μM and 5%–10% measurement uncertainty. We calculated concentrations of particulate Fe from the difference between total and dissolved Fe.

Sulfur compounds

We analyzed concentrations of dissolved H_2S, $S_2O_3^{2-}$, and sulfite (SO_3^{2-}) according to Zopfi et al. (2008). Briefly, 450 μL unfiltered water samples were fixed in a mixture of 25 μM of HEPES-EDTA buffer (pH 8, 500 mM, 50 mM) and 25 μL of ~ 45 mM monobromobimane. After 30 min of incubation protected from light, we stopped the derivatization reaction by adding 50 μL of 312 mM methanesulfonic acid. The samples were stored at −20°C until analysis with reversed-phase high-performance liquid chromatography (RP-HPLC, Dionex) using a LiChrosphere 60RP select B column (125 × 4 mm, 5 μm; Merck) and a Waters 470 scanning fluorescence detector (excitation at 380 nm; detection at 480 nm). In certain cases, H_2S concentrations were determined photometrically through the methylene blue reaction in unfiltered samples, immediately fixed with zinc acetate (0.5% final concentration, w/v) upon collection (Cline 1969). For the analysis of suspended S^0, we filtered 60 mL of water sample through a glass microfiber (GF/F) filter (Whatman) and subsequently stabilized the S^0 on the filter with 2–3 mL of 5% (w/v) zinc acetate solution. The filters were stored at −20°C until analysis. Using 2 mL of HPLC grade methanol, S^0 was extracted overnight from the filters and subsequently quantified by RP-HPLC using a Knauer C18-column (Eurospher II, 100-5 C18 H, 125 × 4 mm) and ultraviolet (UV) detection at 265 nm (Zopfi et al. 2008). Sulfate (SO_4^{2-}) concentrations were analyzed by ion chromatography and UV detection (940 Professional IC Vario, Metrohm).

Methane

We analyzed CH_4 concentrations in November 2016 and October 2017, as described in Su et al. (2023). Briefly, water samples were collected in 120 mL serum bottles, crimp-sealed with butyl rubber stoppers, and a 20 mL air headspace was created before fixing the sample with 5 mL of 12.5 M NaOH. CH_4 concentrations were measured using a gas chromatograph (SRI 8610C, SRI Instruments) with a flame ionization detector.

Turbulent flux calculations

Using the concentration measurements, we calculated turbulent diffusive fluxes of NO_3^-, NH_4^+, H_2S, and CH_4 toward the RTZ (Supporting Information Appendix S1).

DNA extraction, PCR amplification, Illumina sequencing, and data analysis

Filters with collected DNA were stored at −70°C until extraction of DNA using the Fast DNA Spin Kit for Soil (MP Biomedicals). In addition to the 2015–2018 samples, we used samples collected the same way in 2009 and 2010 (*see* Su et al. 2023). The 16S rRNA gene library preparation, amplicon sequencing, and bioinformatic treatment of raw sequences are described in detail in Su et al. (2023). Briefly, the updated Earth Microbiome PCR primers for bacteria and archaea 515F-Y and 926R, targeting the V4 and V5 regions of the 16S rRNA gene, were used for the first PCR (Parada et al. 2016). Library preparation and Illumina MiSeq sequencing was done at the Genomics Facility Basel (D-BSSE ETHZ and Basel University). Amplicon sequence variants (ASVs) were identified by denoising amplicons to zero-radius operational taxonomic units using the UNOISE algorithm in USEARCH v10.0.240 (Edgar 2010, 2013). Finally, we used SINTAX (Edgar 2016) and the SILVA 16S rRNA reference database v138 (Quast et al. 2013) for the taxonomic assignment of ASVs. The details of downstream sequence analyses and statistics can be found in the Supporting Information Appendix 2.

Batch incubation experiments and microbial enrichments

We performed batch incubations with lake water sampled between 2016 and 2018 to investigate NO_3^- reduction with

different electron donors. In 1-L borosilicate bottles with water samples, we introduced a N_2 headspace (~ 130 mL) and purged for 30 min with N_2 to ensure anoxic incubation conditions. Subsequently, we added NO_3^-, NO_3^- and H_2S, or NO_3^- and sodium acetate (NaAc) from sterile anoxic stock solutions. Targeted initial concentrations for NO_3^- and NaAc were 25 μM; for H_2S they ranged between 25 and 100 μM. One bottle was left as a live control treatment without any amendment, and we incubated a dead control with NO_3^- and H_2S, killed with 15 mL 50% (w/v) $ZnCl_2$, to ensure that no abiotic H_2S oxidation was taking place (data not shown). Incubations were carried out at ~ 8°C in the dark with gentle agitation. We monitored the concentrations of dissolved N and S species by taking subsamples (~ 10 mL) at specific time intervals. To prevent contamination with O_2, we initially pressurized the incubation bottles to around 2 bars and used N_2-flushed syringes for sampling. When H_2S was consumed before the complete reduction of NO_3^-, we added additional H_2S (~ 25 μM final concentration). At the end of the experiment, we filtered the remaining water (approximately 300–800 mL) to collect biomass for DNA extraction and sequencing, as described above. This allowed us to identify microbial taxa that responded positively to the different substrate additions. We calculated NO_3^- turnover rates based on the change in NO_3^- concentration over time, using samples from two intervals, (i) the first 2–3 d and (ii) the first 4–5 d of incubation. We tested differences between treatments with a pairwise *t*-test and differences between intervals with an ANOVA. Similarly, we calculated turnover rates for H_2S, S^0, SO_3^{2-}, $S_2O_3^{2-}$, and SO_4^{2-} using samples collected during the first 3–4 d of incubation. A *t*-test was performed on the rates to test for significance.

^{15}N-label incubation experiments

The ^{15}N-label incubation experiments were performed in October 2017 and April 2018 to determine rates of denitrification, anammox, and DNRA at different depths in the water column. We used a modified version of the protocol described in Wenk et al. (2013), adjusted for the additional quantification of $^{15}NH_4^+$. We introduced a 10 mL He headspace to the 160 mL sample vials and purged for 10 min with He to remove potential traces of O_2. Subsequently, we added ^{15}N-NO_3^- tracer from a sterile and anoxic stock solution of 7.5 mM ^{15}N-KNO_3 (99% ^{15}N-KNO_3, Cambridge Isotope Laboratories, Inc.), aiming for an initial $^{15}NO_3^-$ concentration of 25 μM. Additionally, H_2S or Na-acetate (each 25 μM final concentration) was added in the respective treatments (Table 1). All incubations were performed in triplicate in October 2017 and in quintuplicate in April 2018. Incubations were performed in the dark, at ~ 8°C with gentle agitation. Samples for N_2 isotope analysis were collected at five time points (~ 12, 36, 60, 108, and 325 h) by sampling 2 mL of headspace, in exchange with He, using an airtight 3 mL Luer-lock plastic syringe (Braun) with a plastic valve flushed 3 times with

Table 1. Incubation conditions and potential rates determined in ^{15}N-tracer incubation experiments. Values are presented with standard error of means for triplicate or quintuplicate incubations. Percentages refer to the relative contribution of a given process with respect to the combined production of ^{15}N-N_2 and ^{15}N-NH_4^+.

Sampling campaign	Depth	Initial $^{15}NO_3^-$ (μM)	Additional substrate	Denitrification (nmol N-N_2 L^{-1} d^{-1})	Anammox (nmol N-N_2 L^{-1} d^{-1})	DNRA (nmol N-NH_4^+ L^{-1} d^{-1})	Denitrification (%)	Anammox (%)	DNRA (%)
October 2017	95 m	25	—	60.0 ± 13.9	1.5 ± 0.9	0	98	2	0
		25	25 μM acetate	25.5 ± 5.4	1.6 ± 0.7	0	94	6	0
		25	70 μM H_2S	71.0 ± 5.8	0.7 ± 0.4	471.1 ± 25.4	13	0	87
April 2018	95 m	25	—	113.0 ± 65.3	12.0 ± 4.7	142.2 ± 57.5	42	4	53
		25	25 μM acetate	19.4 ± 2.9	1.9 ± 0.9	0	91	9	0
		25	30 μM H_2S	39.1 ± 1.7	0.1 ± 0.0	1139.2 ± 59.9	3	0	97
April 2018	105 m	25	—	28.8 ± 4.2	12.5 ± 2.0	0	70	30	0
		25	25 μM acetate	31.7 ± 3.1	10.7 ± 2.0	161.3 ± 70.7	16	5	79
		25	100 μM H_2S	69.3 ± 3.5	4.5 ± 2.1	1706.6 ± 86.6	4	0	96

He. The samples were stored in 3 mL exetainers after replacing sterile anoxic water with the gas sample. In addition to headspace samples, we took 5-mL liquid samples, filtered them using 0.2 μm membrane filters, and stored them frozen until analysis. The resulting negative pressure in the incubation vials was equilibrated by adding He. We determined $^{15}N\text{-}N_2$ production (m/z 29/28 and 30/28 ratios) via isotope ratio mass spectrometry (IRMS; Flash-EA-ConfloIV-DELTA V Advanced, Thermo Scientific) and calculated the rates of denitrification and anammox according to the isotope pairing equations of (Thamdrup and Dalsgaard 2002) and Thamdrup et al. (2006), where we used only the first three time points. The $^{15}N\text{-}NH_4^+$ samples were transformed to $^{15}N_2$ by oxidation with hypobromite (Risgaard-Petersen et al. 1995) and analyzed as described above. NH_4^+ standards of different concentrations and $^{15}N/^{14}N$ ratios were included in the analysis. We referenced the samples against air N_2 and used the quantified NH_4^+-derived $^{15}N_2$ to assess $^{15}N\text{-}NH_4^+$ concentrations in the liquid sample according to Cojean et al. (2020). DNRA rates were then calculated from the slope of the increase in $^{15}N\text{-}NH_4^+$ concentration over time. Given that anammox rates were low (Table 1), we assumed that the consumption of $^{15}N\text{-}NH_4^+$ produced by DNRA was negligible. For all rates, we estimated the detection limit as 1.5 times the standard error (SE).

Results

Water column characteristics and hydrochemistry

Water column CTD profiles and characteristics are shown in Supporting Information Fig. S1. Water column stability was generally strongest in the subsurface waters, where temperature and density gradients were steepest; no significant density gradient was observed at the RTZ. All O_2 was consumed approximately at a water depth of ~ 80 and 90 m (four selected time points in Fig. 1), which was 35–45 m higher up in the water column compared to 2009 and 2010 (Wenk et al. 2013).

The biweekly O_2 monitoring data from 2015 to 2018 showed highest concentrations between 0 and 20 m during spring and summer, while in late summer and autumn, the water column was generally less oxygenated, with an O_2 depletion at ~ 20 to 30 m (Supporting Information Fig. S2a). Among the sampling dates, when we collected water samples for incubation experiments, April 2018 was the only date with a distinct O_2 peak (up to ~ 500 μM at ~ 15 m) in shallow waters (Supporting Information Fig. S1a). The Chl *a* concentrations in the surface waters were highest in spring and summer (Supporting Information Fig. S2b). The NO_3^- concentrations were highest between 20 and 50 m depth, ranging from 24 to 38 μM. Detailed concentration profiles at the RTZ (Fig. 1; Supporting Information Fig. S3) indicate that NO_3^- decreased to < 0.5 μM within the RTZ. For most time points, NO_2^- did not exceed 0.05 μM in the RTZ. NH_4^+ concentrations started to increase around the depth of O_2 depletion and reached between 15 and 25 μM at ~ 155 m. NH_4^+ and NO_3^- profiles generally overlapped with concentrations of ~ 1–2 μM. H_2S was first detected approximately 15 m below the depth where NO_3^- reached its lowest levels < 0.5 μM (Figs. 1, 2a–c), whereas S^0, the most abundant product among the intermediates of H_2S oxidation, was detectable up to the

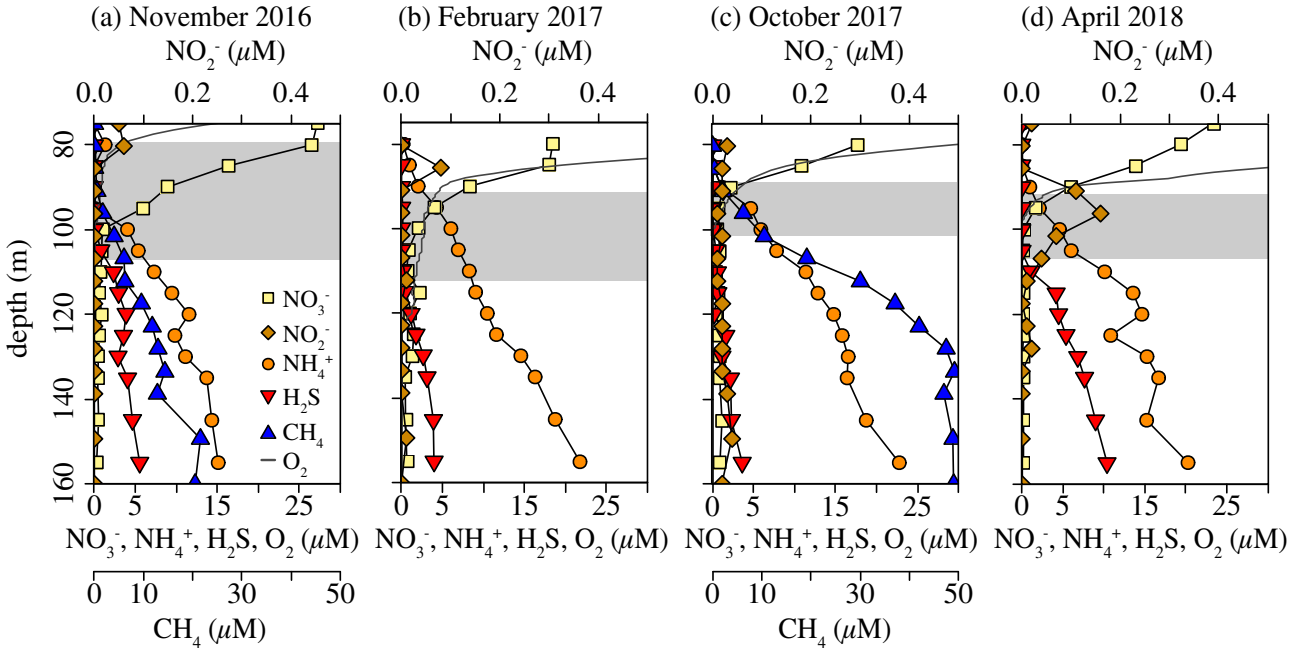

Fig. 1. Concentration profiles at the water column redox transition zone (RTZ) of Lake Lugano's North Basin from four different sampling campaigns. CH_4 was measured only in November 2016 and October 2017. The gray bars indicate the extension of the RTZ.

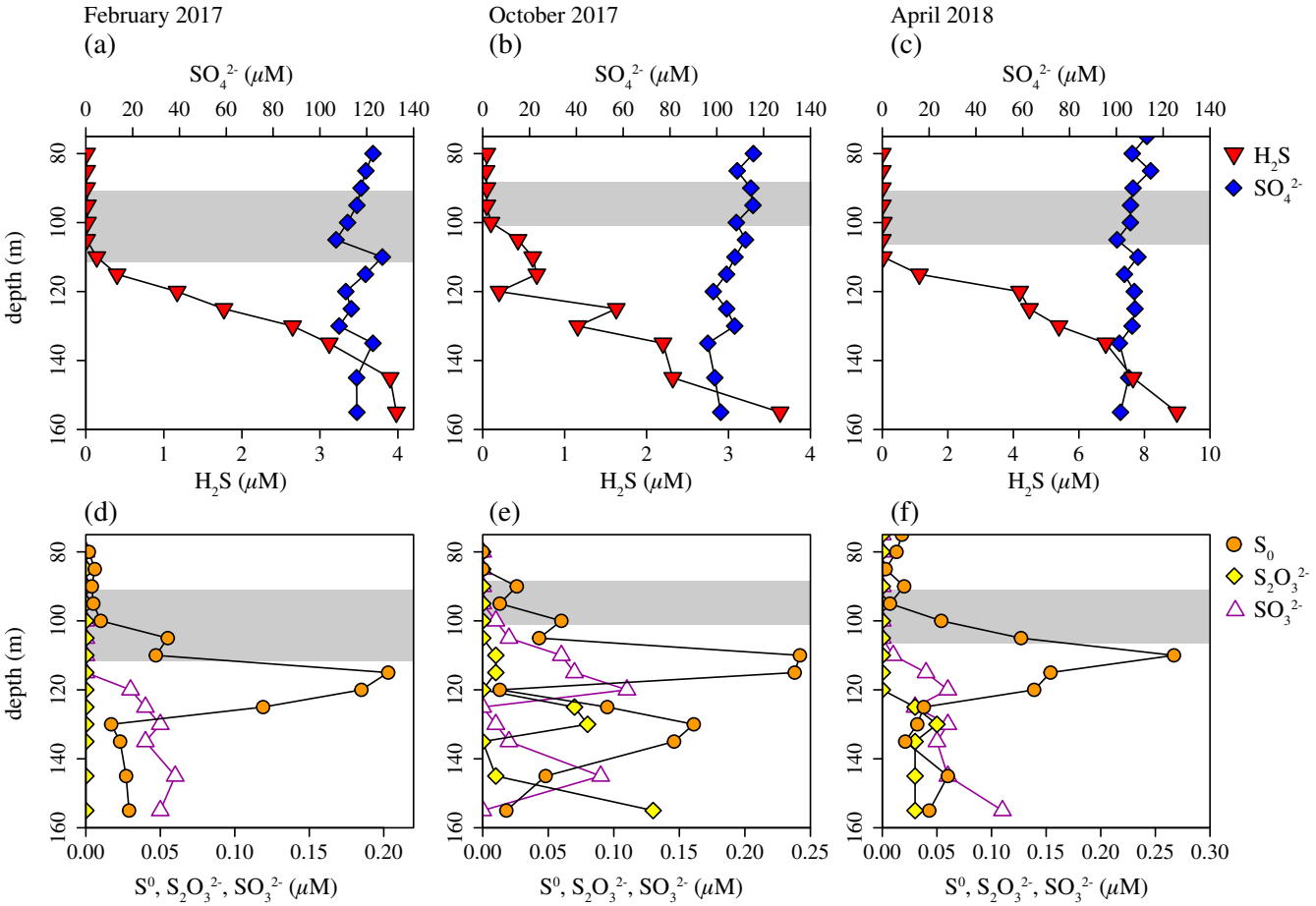

Fig. 2. Depth profiles of sulfur compounds across and below the redox transition zone (RTZ) (gray bars), from February 2017 (**a** + **d**), October 2017 (**b** + **e**), and April 2018 (**c** + **f**).

upper border of the RTZ at levels up to ~ 0.25 μM (Fig. 2d–f). Low SO_3^{2-} and $S_2O_3^{2-}$ concentrations of < 0.15 μM were detected in most of the anoxic water samples. The October 2017 profiles stand out, as S^0, $S_2O_3^{2-}$, and SO_3^{2-} consistently showed two distinct concentration peaks in the anoxic water column. Dissolved Fe^{2+} concentrations rose up to ~ 3 μM at around 160 m depth, while particulate Fe remained below 1 μM, reaching a maximum at 125–130 m in October 2017 and April 2018. CH_4 concentration profiles (November 2016 data have been previously published in Su et al. 2023; Fig. 1) clearly overlapped with NO_3^- profiles. Below the RTZ, CH_4 concentrations increased to up to ~ 50 μM (e.g., October 2017). Turbulent diffusive solute fluxes toward the RTZ between 2015 and 2018 were on average 828 ± 315 SD μmol for NO_3^- m^{-2} d^{-1}, 379 ± 122 SD μmol for NH_4^+ m^{-2} d^{-1}, 199 ± 87 SD μmol for H_2S m^{-2} d^{-1}, and 882 ± 597 SD μmol for CH_4 m^{-2} d^{-1} (Supporting Information Table S3).

Microbial community structures

The 16S rRNA gene sequencing revealed differences between the microbial communities in the oxic water column just above the RTZ, within the RTZ, and in the anoxic water below the RTZ regarding their alpha and beta diversities (Fig. 3). The observed ASV richness (Kruskal–Wallis test; $\chi^2 = 76.5$, df = 2, $p < 0.001$) was significantly higher in the anoxic water below the RTZ compared to the oxic water layer (Dunn's test; $Z = 6.2$, $p_{adj} < 0.001$) and the RTZ (Dunn's test, $Z = 7.6$, $p_{adj} < 0.001$). ASV richness increased with time during the multiannual survey of the microbial community structure in the water column (Supporting Information Fig. S4), especially in the anoxic water below the RTZ (Pearson correlation coefficient; $t = 3.0$, $n = 68$, $r = 0.34$). The Shannon diversity index (Kruskal–Wallis test; $\chi^2 = 18.8$, df = 2, $p < 0.001$), which quantifies both richness and evenness, was higher in the oxic water compared to the RTZ (Dunn's test; $Z = 4.0$, $p_{adj} < 0.001$) and the anoxic water layer (Dunn's test; $Z = -4.1$, $p_{adj} < 0.001$). The community structure in the oxic water column seems to be more evenly distributed than in the RTZ and the anoxic zone. Particularly, the communities in the anoxic layer show a high richness (i.e., many different ASVs) but lower Shannon diversity, indicating a community with few high-abundance and many very low-abundance taxa.

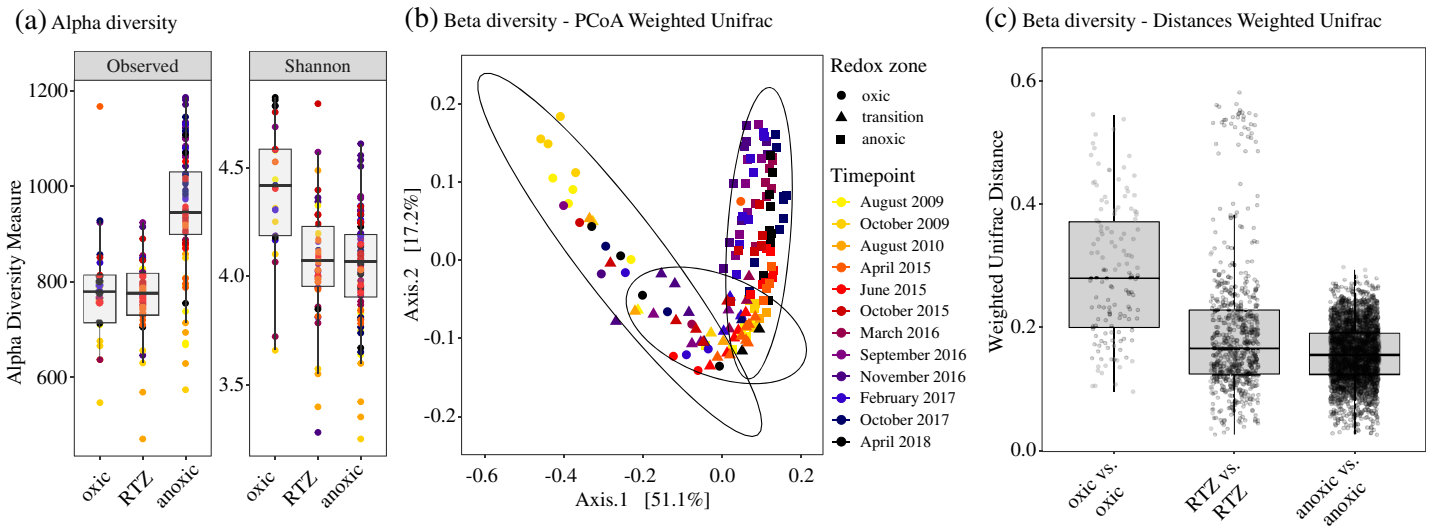

Fig. 3. Characterization of the microbial communities in the water column of Lake Lugano's North Basin depending on redox regime ("oxic," redox transition zone: "RTZ," "anoxic") and/or sampling time point using 16S rRNA gene amplicon sequencing variant (ASV) data from 2009 to 2018. (**a**) Observed ASV richness and Shannon diversity and (**b**) principal coordinate analysis (PCoA) of weighted UniFrac distances, and (**c**) weighted UniFrac distances of microbial community structures within the three distinct redox zones.

The PCoA showed that the microbial community structures followed the three redox zones, although the transitions were gradual and zones were overlapping (Fig. 3b). The community structures in the three defined redox zones were significantly different from each other (PERMANOVA; $F_{2,116} = 114.3$, $R^2 = 0.38$, $p < 0.001$). Post hoc pairwise comparisons showed significant differences between all zone pairs: oxic vs. RTZ ($F_{1,65} = 18.2$, $R^2 = 0.22$, $p < 0.001$), oxic vs. anoxic ($F_{1,107} = 77.5$, $R^2 = 0.42$, $p < 0.001$), and RTZ vs. anoxic ($F_{1,124} = 36.6$, $R^2 = 0.23$, $p < 0.001$). Furthermore, significant differences were observed across time points (PERMANOVA; $F_{11,116} = 13.3$, $R^2 = 0.24$, $p < 0.001$) and in the interaction between time points and redox zones (PERMANOVA; $F_{21,116} = 5.5$, $R^2 = 0.19$, $p < 0.001$). The microbial community structure below the RTZ exhibited the least variability over time (average distance 0.13), significantly lower than in the oxic zone (0.23; PERMDISP ANOVA: $F_{2,148} = 20.97$, $p < 0.001$; post hoc oxic vs. anoxic zone: $p < 0.001$). Pairwise Weighted UniFrac distances between samples within a specific redox zone are presented in Fig. 3c.

Phylogenetic analysis of 16S rRNA gene amplicons revealed Proteobacteria, Bacteroidota, Actinobacteriota, Chloroflexi, and Crenarchaeota as the dominant phyla (Supporting Information Fig. S5a), and Actinobacteria, Bacteroidia, and Gammaproteobacteria as the dominant classes (Supporting Information Fig. S5b). Below the RTZ, the relative abundance of Desulfobacterota and Nanoarchaeota increased with depth. The composition of the microbial community (Supporting Information Fig. S6) varied more in the oxic water column than in the RTZ and the anoxic water column. ASVs linked to N- and S-cycling are summarized in Supporting Information Table S2 and Supporting Information Figs. S7–S11; vertical distribution profiles of key taxa are shown in Fig. 4. We detected the NH_4^+-oxidizing archaeon *Candidatus* Nitrosopumilus, the NH_4^+-oxidizing bacteria *Nitrosospira* and *Nitrosomonas*, and the NO_2^--oxidizing bacterium *Nitrospira* with highest relative abundances at low O_2 conditions above the RTZ (Fig. 4a–c). Furthermore, we detected the anammox-associated family Brocadiaceae (Fig. 4d). We also identified several taxa capable of N reduction with maximum relative abundances within the RTZ (Fig. 4e–j), including organotrophic N reducers, such as *Denitratisoma*, S-oxidizing N reducers such as *Sulfuritalea*, and CH_4-oxidizing *Ca.* Methylomirabilis. A diverse community of taxa commonly known for reducing SO_4^{2-} and/or other sulfur compounds (e.g., S^0, $S_2O_3^{2-}$) was present. These "S-reducers" belonged mostly to the Desulfobacterota (formerly Deltaproteobacteria), such as *Desulfobacca*, *Desulfocapsa* (Fig. 4k,l), or *Desulfovibrio*. In addition, we identified putative S-reducing Firmicutes, including *Desulfosporosinus* and *Desulfurispora*. Some of these potential S-reducers, such as *Desulfosporosinus* (Supporting Information Fig. S11a) and *Desulfomonile* (Supporting Information Fig. S11g), exhibited distinct abundance peaks in and/or below the RTZ.

Nitrogen transformation incubation experiments

In the unlabeled incubations (Fig. 5) amended solely with NO_3^-, NO_3^- consumption was generally incomplete, with decreases of 3–11 μM NO_3^-. Most of the NO_3^- was only converted to NO_2^- (Fig. 5d). Complete removal of NO_3^- (and subsequently NO_2^-) occurred in only one of the duplicate incubations in February 2017 and April 2018 (Fig. 5a,d).

The addition of acetate led to complete reduction of NO_3^- within 4–5 d, following an initial lag phase (Fig. 5b). The

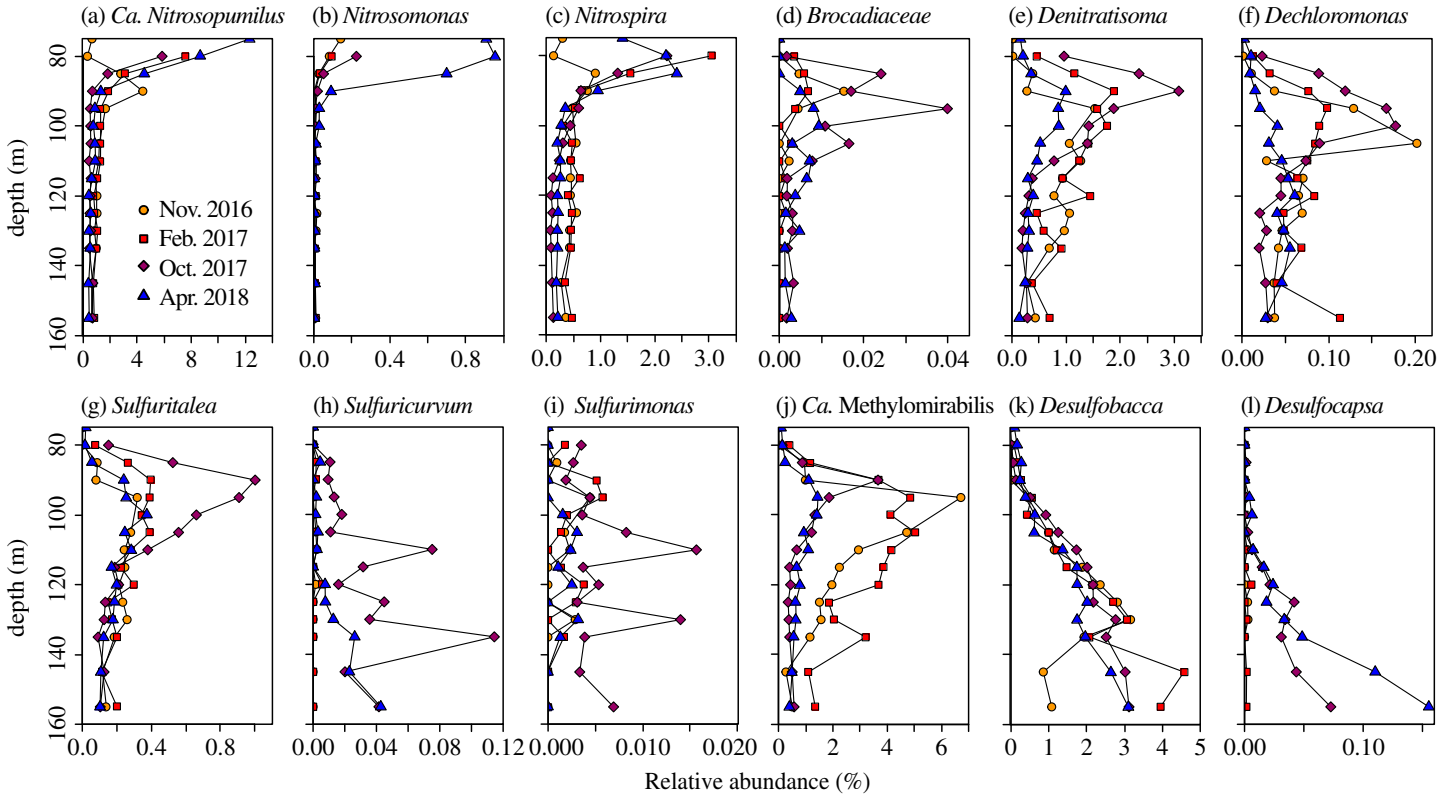

Fig. 4. Depth distribution and temporal variability of the main taxa of N and S cycling microorganisms. Selected nitrifiers (**a**–**c**), anammox-performing bacteria (**d**), organotrophic- (**e**, **f**), sulfidotrophic- (**g**–**i**) and methanotrophic N reducers (**j**), and S-reducers (**k**, **l**) are presented. Data are based on relative abundances of 16S rRNA gene amplicons.

addition of H_2S caused complete NO_3^- consumption within ~ 10–30 d (Fig. 5c). Transient NO_2^- accumulation was observed in the incubations with either acetate or H_2S (Fig. 5e,f). The NO_3^- reduction rates during the first 2–3 d of incubation (Supporting Information Fig. S12a) were highest for the $NO_3^- + H_2S$ treatment with 1.4 ± 0.3 SE μmol NO_3^- L^{-1} d^{-1}. For the NO_3^--only (0.6 ± 0.2 SE μmol NO_3^- L^{-1} d^{-1}) and the NO_3^- + acetate treatment (0.9 ± 0.4 SE μmol N-NO_3^- L^{-1} d^{-1}), initial NO_3^- reduction rates were lower. Whereas after the initial phase (Supporting Information Fig. S9b) NO_3^- consumption rates in the NO_3^--only treatment (0.7 ± 0.4 SE μmol NO_3^- L^{-1} d^{-1}) and the $NO_3^- + H_2S$ treatment (1.7 ± 0.3 SE μmol NO_3^- L^{-1} d^{-1}) remained similar, NO_3^- consumption rates in the NO_3^- + acetate treatment increased to 3.2 ± 0.6 SE μmol NO_3^- L^{-1} d^{-1} (ANOVA; $F_{1,22} = 9.8$, $R^2 = 0.31$, $p = 0.005$). During the incubations, H_2S was consumed and S^0 and $S_2O_3^{2-}$ accumulated, but no substantial amounts of SO_4^{2-} were produced (Supporting Information Table S4; Supporting Information Fig. S13).

^{15}N incubation rate measurements

In the ^{15}N-incubation experiments conducted in October 2017 and April 2018 (example in Supporting Information Fig. S14), denitrification rates ranged between 28.8 and 113.0 nmol N-N_2 L^{-1} d^{-1} in the treatments with $^{15}NO_3^-$ and no added electron donors (Table 1). Hence, N_2 production rates were almost an order of magnitude lower than NO_3^- consumption rates determined in parallel unlabeled experiments, likely due to NO_2^-accumulation, which also occurred in the unlabeled incubations (Fig. 5d). Amended acetate and H_2S did not significantly change denitrification rates (ANOVA; $F_{2,6} = 2.1$, $R^2 = 0.41$, $p = 0.21$), which ranged between 19.4 and 31.7 nmol N-N_2 L^{-1} d^{-1} for the $^{15}NO_3^-$ + acetate treatment and between 39.1 and 71.0 nmol N-N_2 L^{-1} d^{-1} for the $^{15}NO_3^- + H_2S$ treatment. Qualitatively consistent with the observed NO_3^- reduction dynamics in the unlabeled incubations, acetate-supported $^{30}N_2$ production started only after a lag phase of more than 3 d (Supporting Information Fig. S14e). While in the $^{15}NO_3^-$ and $^{15}NO_3^-$ + acetate incubations, DNRA rates were undetectable or < 150 nmol ^{15}N-NH_4^+ L^{-1} d^{-1}, the addition of H_2S resulted in high DNRA rates between 471.1 and 1706.6 nmol ^{15}N-NH_4^+ L^{-1} d^{-1}, representing 87% to 97% of the total ^{15}N-N_2 + ^{15}N-NH_4^+ produced. Anammox rates were low in all treatments, ranging from 0.1 up to 12.5 nmol ^{15}N-N_2 L^{-1} d^{-1}. They accounted for 0% to 30% (but mostly < 10%; Table 1) of the produced ^{15}N-N_2 + ^{15}N-NH_4^+, without any significant differences between treatments (ANOVA; $F_{2,6} = 1.5$, $R^2 = 0.33$, $p = 0.30$), and were

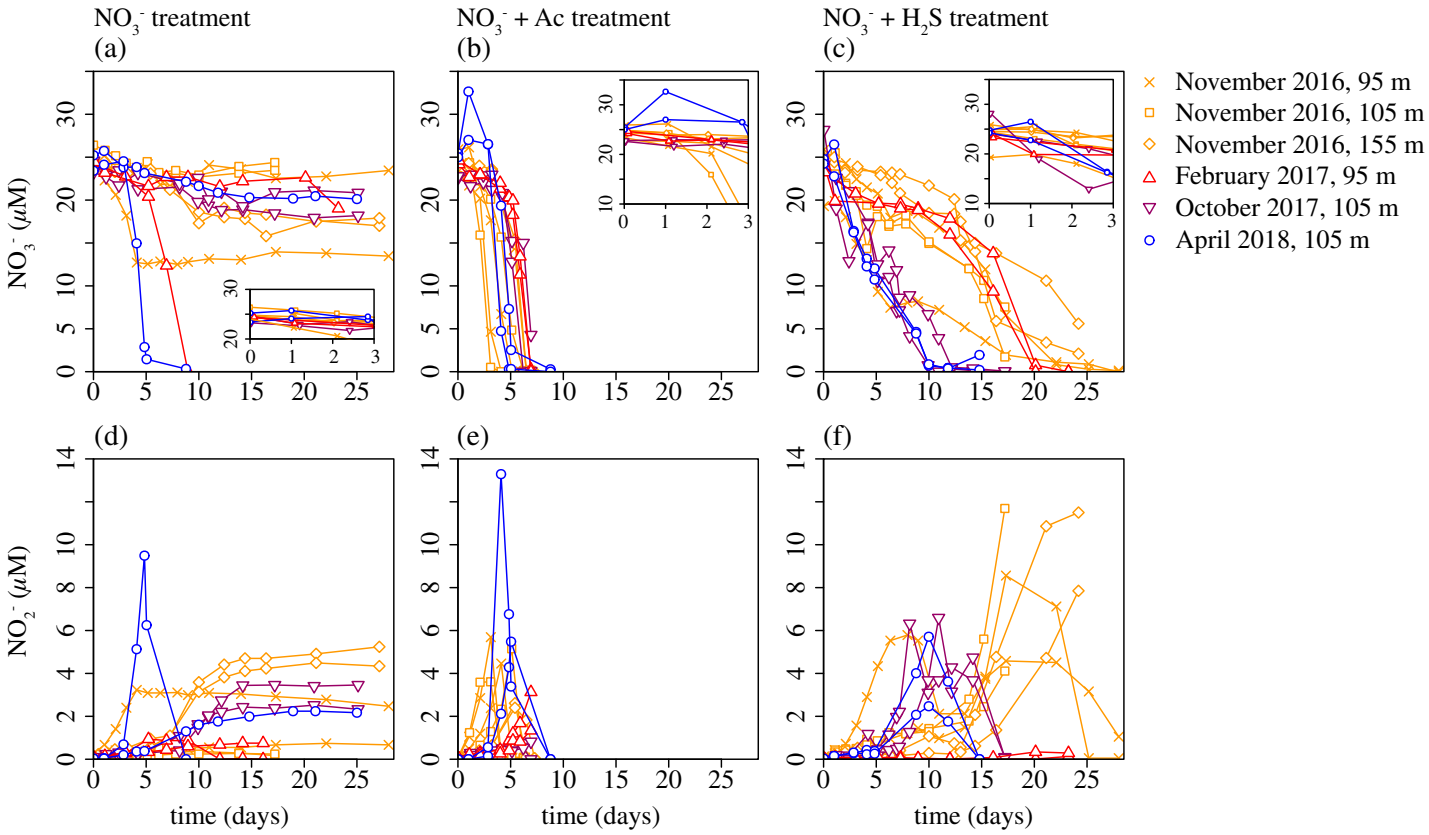

Fig. 5. Concentrations of NO_3^- (**a–c**) and NO_2^- (**d–f**) in unlabeled incubation experiments performed with water samples from the redox transition zone (RTZ) in Lake Lugano's North Basin, with added NO_3^- (a, d), NO_3^- and acetate (b, e), or NO_3^- and H_2S (c, f). Inserts show NO_3^- concentration changes during the first 3 d of the experiment.

not considered further in the discussion. In experiments where we detected DNRA, some of the produced ^{15}N-NH_4^+ may have been subsequently consumed by anammox, potentially leading to an underestimation of DNRA rates.

Discussion

The results from unlabeled and ^{15}N-label incubation experiments and 16S rRNA gene sequencing data provide conclusive evidence for active N-cycling around the RTZ, coupled to the S- and C-cycles. The overlapping concentration profiles of NH_4^+ and NO_3^- with complete consumption of both substrates within the RTZ suggest that NH_4^+ oxidation (aerobic and anaerobic) and NO_3^- reduction take place simultaneously and in close vicinity. In the following sections, we discuss the relevance of H_2S and organic compounds for N reduction, the N reduction pathway they fuel, as well as potential microbial players involved. The scope for CH_4-dependent N reduction has been discussed previously in Su et al. (2023), but its quantitative contribution remains uncertain and requires further experimental investigation (Supporting Information Appendix 3). We therefore focus here on the closely coupled (and possibly cryptic) interactions between N- and S-cycling within the RTZ.

Role of organic electron donors for N reduction

Limited availability of reactive C_{org} for canonical denitrification was indicated in the unlabeled incubation experiments, where only a small fraction of the added NO_3^- was reduced. The ^{15}N-label incubation experiments confirm low denitrification activity, even during the algal bloom period in April 2018 (primary production 46.5 g C m^{-2} $month^{-1}$; www.cipais.org). Consistent with a strong decline of dissolved O_2 below the primary production zone in summer and autumn (Supporting Information Fig. S1a), it appears that a substantial fraction of the freshly produced OM is metabolized before reaching the RTZ at 80–110 m depth. In contrast to most known meromictic systems, the RTZ in Lake Lugano's North Basin is not associated with a strong density gradient capable of trapping detrital C_{org}. As a result, C_{org} particles likely pass through the RTZ unimpeded (Alldredge and Crocker 1995). This

suggests that the sustained low availability of C_{org} in the RTZ may constrain heterotrophic N reduction throughout the year.

We note that our $^{15}NO_3^-$ addition experiments without any additional electron donors, while consistent with previous reports by Wenk et al. (2014), might slightly underestimate the in situ rates of denitrification because volatile electron donors such as CH_4 and H_2S were removed during the purging step required to create anoxic conditions. Additionally, the low rates may reflect that large particles can sink below the Niskin bottle nozzle and therefore are not captured in the water used for the incubations (Gardner 1977; Suter et al. 2017). Nevertheless, denitrification rates in Lake Lugano's North Basin (up to 113 nmol N-N_2 L^{-1} d^{-1}) are at least one order of magnitude lower than those reported for several other lakes (Supporting Information Table S1). Potential explanations include shallower RTZs, as observed in Wintergreen Lake (Burgin et al. 2012), or deep secondary Chl *a* maxima, as reported for Lake Tanganyika (Ehrenfels et al. 2023). However, the underlying causes for the low observed rates in Lake Lugano's North Basin remain to be investigated.

Sulfur-dependent N reduction

We demonstrate a high potential of S-dependent DNRA in the ^{15}N-label experiments with up to 1707 nmol NH_4^+ L^{-1} d^{-1} and a comparatively low potential of S-dependent denitrification (up to 71 nmol N-N_2 L^{-1} d^{-1}). Active S-dependent N reduction is also indicated by the presence of intermediates of S-oxidation, especially of S^0 and $S_2O_3^{2-}$, which accumulated in the unlabeled incubation experiments and were present in situ with up to ~ 0.25 μM S^0 and ~ 0.10 μM $S_2O_3^{2-}$. The ambient NO_3^- concentrations at the sampled depths were low, a condition generally thought to favor DNRA over denitrification, particularly in the presence of C_{org} or reduced sulfur compounds (Kelso et al. 1997; Strohm et al. 2007; Dong et al. 2011). However, H_2S concentrations were undetectable at the depths sampled for incubations, and high DNRA rates were only observed upon the addition of H_2S and NO_3^-. Hence, the in-situ dominance of S-dependent DNRA in the water column remains uncertain. Future studies could address this by quantifying the expression of the *nrfA*, a molecular marker for DNRA (Pandey et al. 2020), in RNA extracts.

Measurements from other lakes have revealed substantial differences in both the relative and absolute importance of DNRA and denitrification, whether coupled to S oxidation or C_{org} oxidation. For example, in Lake Kivu (Roland et al. 2018) and in Wintergreen Lake (Burgin et al. 2012), both organotrophic and S-dependent forms of denitrification and DNRA (partly coupled to S-oxidation) have been detected. Yet, in these systems, DNRA accounted for only up to ~ 15% of the total ^{15}N-turnover, while our data suggest that in Lake Lugano's North Basin DNRA may contribute up to 97%, indicating a potentially dominant role under the conditions tested.

The 16S rRNA gene sequencing analysis revealed bacterial genera in the RTZ, which likely perform S-dependent N reduction, like *Sulfuritalea*, *Sulfuricurvum*, and *Sulfurimonas*. We speculate that the N-reducing *Dechloromonas*, which also harbors genes for the Sox sulfur-oxidation enzyme system (Luo et al. 2018) and proliferated in the unlabeled incubations with added NO_3^- and H_2S (Tischer et al. 2025), may also perform S-oxidation in the RTZ in addition to organotrophic denitrification.

Based on 16S rRNA gene sequencing data, the observed sulfur speciation in the water column, and the H_2S-addition experiments, we suggest that the most active zone for S-oxidizing N reducers may be a "cryptic-sulfur-cycling" zone, where S-oxidation and reduction are so tightly coupled that free H_2S is undetectable. Cryptic sulfur cycling has already been reported for marine oxygen minimum zones, albeit with much lower rates (Canfield et al. 2010; Callbeck et al. 2018). In the 10–40 m thick RTZ of Lake Lugano's North Basin, we detected S^0, a high-rate potential for S-dependent DNRA, and maximum relative abundances of *Sulfuritalea*. We argue, therefore, that H_2S diffusing toward the RTZ is quantitatively oxidized by NO_3^--reducing microorganisms performing DNRA. The volumetric H_2S oxidation rate that would be required to match the observed flux of H_2S toward the RTZ (85–304 μmol d^{-1} m^{-2}) was, on average, 0.013 μmol H_2S L^{-1} d^{-1} (assuming a 15 m thick layer of S-dependent denitrification activity; Supporting Information Table S3). However, H_2S consumption in the unlabeled anoxic incubation experiments averaged 4.6 μmol H_2S L^{-1} d^{-1}, over 350-times higher than the rate needed to completely oxidize the upward-diffusing H_2S in the water column, indicating a substantial potential for H_2S utilization. In addition, the presence of a S-reducing microbial community, dominated by *Desulfobacca* (Fig. 4k), underscores the potential for in-situ H_2S production within and below the RTZ. This H_2S may be rapidly consumed by S-oxidizing microorganisms, potentially supporting cryptic S-dependent DNRA and, to a lesser extent, S-dependent denitrification.

Cryptic N cycling through nitrification and DNRA coupling

We suggest that N recycling via S-dependent DNRA and nitrification is a key mechanism in the RTZ of Lake Lugano's North Basin, which helps to retain bioavailable N. Activity of NH_4^+ and NO_2^- oxidation close to the oxic-anoxic interface is evidenced by a community of abundant nitrifiers, including *Ca.* Nitrosopumilus. This archaeal NH_4^+ oxidizer is common in marine environments (Könneke et al. 2005) but has also been observed in deep oligotrophic freshwater bodies such as Lake Constance (Klotz et al. 2022). Although nitrification rates remain to be quantified, maximum relative abundances close to the upper boundary of the RTZ indicate that *Nitrosomonas* or *Nitrosospira* encounter excellent conditions for nitrification,

with replete O_2 and a constant supply of NH_4^+. Studies on stratified lakes have evidenced active nitrification within the respective RTZs (Christofi et al. 1981; Pajares et al. 2017). More specifically, in the RTZ of a monomictic tropical lake, Pajares et al. (2017) demonstrated the co-occurrence of nitrification, DNRA, and denitrification genes, highlighting the importance of internal N recycling in the lake.

Nitrification in the RTZ of Lake Lugano's North Basin is likely more important than previously reported by Wenk et al. (2013), who interpreted non-overlapping profiles of O_2 and NH_4^+ as evidence that NH_4^+ oxidation occurs primarily under anoxic conditions, driven by anammox bacteria. However, overlapping O_2 and NH_4^+ concentration profiles observed for 2015–2018, recent dual NO_3^- N and O isotope data (Tischer et al. 2025), and a community shift of nitrifiers, including *Nitrosospira* and representatives of the Nitrosomonadaceae (Supporting Information Table S2), suggest an increased role of nitrification within the RTZ.

Independent of the relatively low turbulent-diffusive fluxes of N compounds toward the RTZ (Supporting Information Table S3), the overall N turnover may be quite high, yet cryptic, due to efficient recycling between the NH_4^+ and NO_3^- pools via DNRA and nitrification. Indeed, an average net consumption rate of 0.055 μmol NO_3^- L^{-1} d^{-1} would have been necessary to match the observed NO_3^- flux toward the RTZ. In the NO_3^--only treatment of the unlabeled incubations, however, potential NO_3^- reduction rates were much higher (average 0.7 μmol NO_3^- L^{-1} d^{-1}), suggesting that the flux-based rates underestimate the potential for NO_3^- reduction and that NO_3^- reduction is closely coupled to microaerobic NO_3^- regeneration. The latter, in turn,

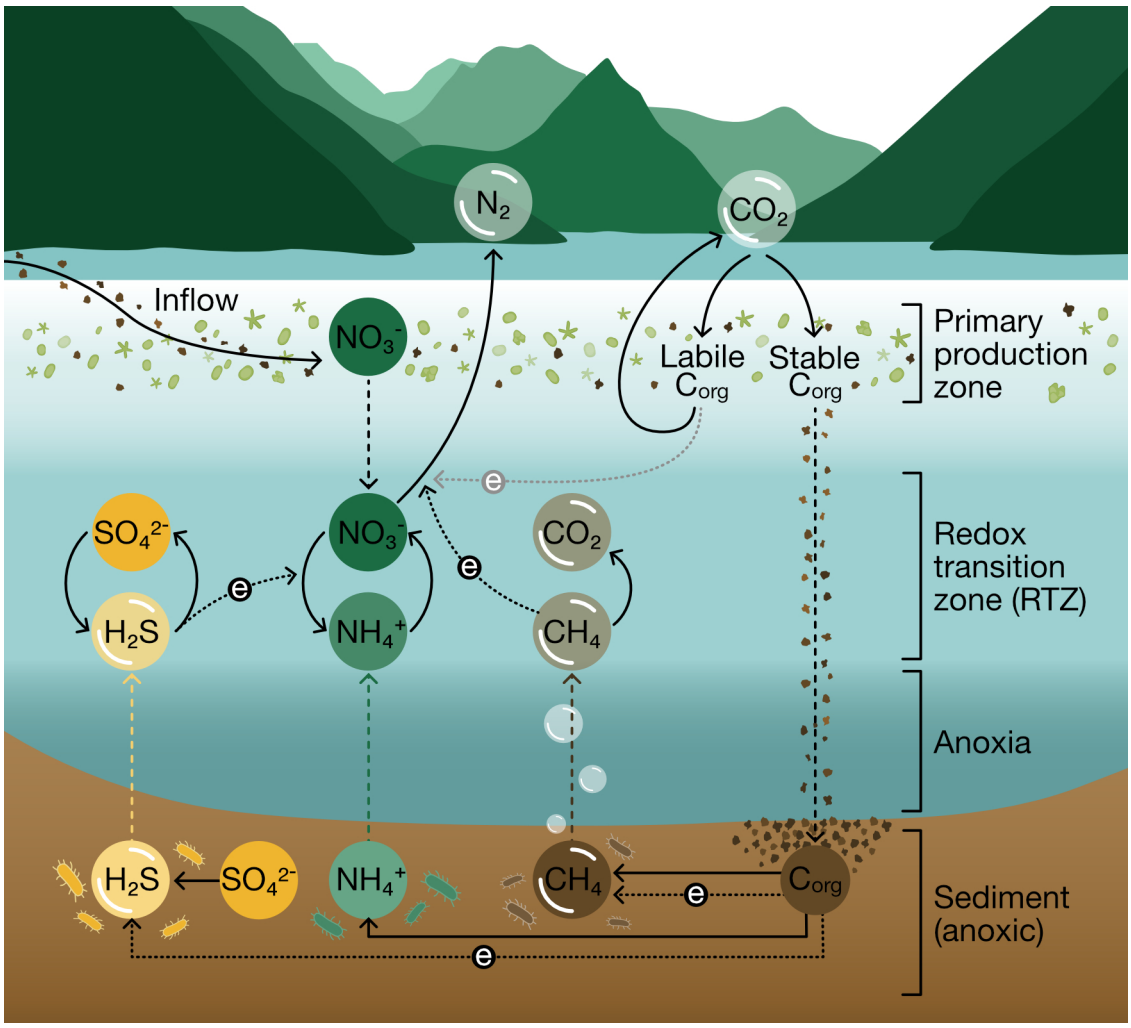

Fig. 6. Schematic illustration of proposed N formation processes in Lake Lugano's North Basin coupled to the S and C cycles. Solid lines indicate transformation processes; dashed lines indicate transport processes or symbolize the flow of electrons. Accessible fractions of fresh organic carbon (labile C_{org}) are mostly degraded in the oxic water column, while the less accessible or more stable fractions (stable C_{org}) are incompletely oxidized and sink to the sediment, where they are metabolized. H_2S, CH_4, along with NH_4^+, steadily diffuse upward to the redox transition zone (RTZ), where they serve as continuous electron sources for denitrification and dissimilatory nitrate reduction to ammonium (DNRA).

may be supported by DNRA, especially by S-dependent DNRA. Cryptic N cycling, that is, without measurable intermediates as NO_2^- or NH_4^+, has been demonstrated in oxic riverbeds (Ouyang et al. 2021). In addition, Lam et al. (2009) demonstrated that a substantial fraction of anammox in the Peruvian oxygen minimum zone is supported by DNRA, without significant accumulation of NH_4^+. In the present-day Lake Lugano North Basin, anammox arguably plays a subordinate role. Here, we suggest a close coupling between DNRA, nitrification, and denitrification that efficiently turns over fixed N and eliminates parts of it as N_2. As with the "cryptic S cycle," we propose a closely linked "cryptic N turnover" involving S-dependent denitrification and DNRA in the RTZ.

Electron donors from sediment fuel N cycling at the RTZ

We argue that N reduction in the North Basin of Lake Lugano is mainly driven by the constant supply of H_2S and CH_4, as conceptualized in Fig. 6. As discussed above, we suggest that most of the C_{org} from primary production is either already degraded in the upper oxic water column or is not readily available as an electron donor in the RTZ. Instead, the accumulating C_{org} in the permanently anoxic lake sediments is further degraded through fermentation, SO_4^{2-} reduction, and methanogenesis, transferring electrons to the benthic H_2S and CH_4 pools (Blees et al. 2014). Microorganisms in the sediment are more abundant and more diverse than those in the water column (Bartosiewicz et al. 2024). Moreover, they have virtually unlimited time to adapt their metabolism and exploit specific organic compounds. In this context, the sediments and their natural microbial communities can be viewed as an "electron donor refinery," converting a non-steady flux of poorly accessible electron donor compounds settling from the water column into sustained H_2S and CH_4 production. These metabolites then diffuse out of the sediments toward the RTZ, where they serve as continuous—and mostly season-independent—electron donors for chemolithotrophic and CH_4-dependent N reduction, respectively. The sustained benthic flux of reduced substrates thus supports the establishment of a stable community of N- and S-cycling microorganisms, structured along a spatial sequence from oxic to low O_2 to anoxic conditions, including key taxa such as nitrifying *Ca.* Nitrosopumilus, *Nitrosomonas*, and *Nitrospira* and N reducing *Denitratisoma*, *Sulfuritalea*, and *Ca.* Methylomirabilis. Microbial community composition within these guilds showed little variation over the course of this study, likely due to the stable environmental conditions and reduced grazing pressure in the lower part of the RTZ and anoxic water layer. We propose that the low but continuous supply of H_2S and CH_4 ultimately underpins the dominance of S- and possibly CH_4-driven NO_3^-/NO_2^- reduction over canonical organotrophic denitrification within the RTZ of Lake Lugano's North Basin.

Conclusions and implications

We investigated the cycling and removal of fixed N within the RTZ of Lake Lugano's North Basin and uncovered a complex interplay of oxidative and reductive N transformation processes. We provide evidence that this meromictic basin, with its deep RTZ, fosters conditions that favor S- and CH_4-driven N reduction over canonical organotrophic denitrification. Nitrification, denitrification, DNRA, and transformation of S species seem to occur in the same water mass, potentially supporting interactive and largely "cryptic" S- and N-cycling. The coupling and partitioning of the different NO_3^--transforming metabolisms determine whether fixed-N is recycled and remains in the system or is removed from it. Because DNRA (and nitrification), unlike denitrification, retains reactive N in the environment, our findings may have important implications for the N budget of Lake Lugano's North Basin. More than 50 yr ago, high inputs of P and N shifted the lake into a meromictic and meso-eutrophic state. Despite a substantial reduction of external P inputs over the last 40 yr (Barbieri and Mosello 1992), the trophic state of the lake has only weakly improved (Lepori et al. 2018). The relatively low fixed-N removal potential in the North Basin, coupled with efficient internal N cycling via DNRA, might contribute to maintaining elevated NO_3^- levels in the water column, thereby slowing down the restoration process of the lake.

Author Contributions

Jakob Zopfi and Moritz F. Lehmann conceived the research project. Jana Tischer, Jakob Zopfi, and Moritz F. Lehmann conceptualized research and experimental design. Jana Tischer, Jakob Zopfi, Moritz F. Lehmann, Guangyi Su, and Fabio Lepori conducted sampling campaigns and contributed to the data acquisition of physicochemical parameters in the water column of Lake Lugano. The lake water incubation experiments were conducted by Jana Tischer and analyzed by Jana Tischer and Jakob Zopfi. Jana Tischer, Jakob Zopfi, and Guangyi Su carried out the data analysis of 16S rRNA sequencing data. Jana Tischer wrote the paper, with substantial input from Jakob Zopfi, Moritz F. Lehmann, Guangyi Su, and Fabio Lepori. Jana Tischer, Jakob Zopfi, and Moritz F. Lehmann are accountable for the integrity of the data, analysis, and presentation of the findings.

Acknowledgments

We thank Marco Simona, Stefano Beatrizotti, Adeline Cojean-Egger, Maciej Bartosiewicz, and Lea Steinle for their help during the sampling campaigns on Lake Lugano. Long-term O_2, NO_3^-, and primary productivity data were generated within a research program funded by the Dipartimento del Territorio (Department of Environment) of the Canton of Ticino, Switzerland, and the International Commission for the Protection of Italian-Swiss Waters (CIPAIS). Jean-Claude Walser from the Genetic Diversity Center (ETHZ) is thanked for bioinformatic support. We are also grateful to Thomas Kuhn and Judith Kobler for providing technical support in the

laboratory. The research was funded by the Swiss National Science Foundation project 153055 granted to Jakob Zopfi and Moritz F. Lehmann. Open access publishing facilitated by Universitat Basel, as part of the Wiley - Universitat Basel agreement via the Consortium Of Swiss Academic Libraries.

Conflicts of Interest

None declared.

Data Availability Statement

Water column chemistry and experimental data are available through the PANGAEA data repository (https://doi.pangaea.de/10.1594/PANGAEA.977622, https://doi.pangaea.de/10.1594/PANGAEA.977623, https://doi.pangaea.de/10.1594/PANGAEA.977624, https://doi.pangaea.de/10.1594/PANGAEA.977625, https://doi.pangaea.de/10.1594/PANGAEA.977626). Treated 16S rRNA gene sequences (ASV) are deposited at the Zenodo repository (https://doi.org/10.5281/zenodo.14885067). Raw sequence data are made available at NCBI under the BioProjectID PRJNA772618 with the accession numbers SAMN47302940 through SAMN47303110.

References

Alldredge, A. L., and K. M. Crocker. 1995. "Why Do Sinking Mucilage Aggregates Accumulate in the Water Column?" *Science of the Total Environment* 165: 15–22. https://doi.org/10.1016/0048-9697(95)04539-D.

Barbieri, A., and R. Mosello. 1992. "Chemistry and Trophic Evolution of Lake Lugano in Relation to Nutrient Budget." *Aquatic Sciences* 54: 219–237. https://doi.org/10.1007/BF00878138.

Bartosiewicz, M., A. Przytulska, A. Birkholz, J. Zopfi, and M. F. Lehmann. 2024. "Controls and Significance of Priming Effects in Lake Sediments." *Global Change Biology* 30: e17076. https://doi.org/10.1111/GCB.17076.

Blees, J., H. Niemann, C. B. Wenk, et al. 2014. "Micro-Aerobic Bacterial Methane Oxidation in the Chemocline and Anoxic Water Column of Deep South-Alpine Lake Lugano (Switzerland)." *Limnology and Oceanography* 59: 311–324. https://doi.org/10.4319/lo.2014.59.2.0311.

Braman, R. S., and S. A. Hendrix. 1989. "Nanogram Nitrite and Nitrate Determination in Environmental and Biological Materials by Vanadium(III) Reduction With Chemiluminescence Detection." *Analytical Chemistry* 61: 2715–2718. https://doi.org/10.1021/ac00199a007.

Brunet, R., and L. Garcia-Gil. 1996. "Sulfide-Induced Dissimilatory Nitrate Reduction to Ammonia in Anaerobic Freshwater Sediments." *FEMS Microbiology Ecology* 21: 131–138. https://doi.org/10.1016/0168-6496(96)00051-7.

Burgin, A., S. Hamilton, S. Jones, and J. Lennon. 2012. "Denitrification by Sulfur-Oxidizing Bacteria in a Eutrophic Lake." *Aquatic Microbial Ecology* 66: 283–293. https://doi.org/10.3354/ame01574.

Burgin, A. J., and S. K. Hamilton. 2007. "Have we Overemphasized the Role of Denititrification in Aquatic Ecosystems? A Review of Nitrate Removal Pathways." *Frontiers in Ecology and the Environment* 5: 89–96. https://doi.org/10.1890/1540-9295(2007)5[89:HWOTRO]2.0.CO;2.

Callbeck, C. M., G. Lavik, T. G. Ferdelmann, et al. 2018. "Oxygen Minimum Zone Cryptic Sulfur Cycling Sustained by Offshore Transport of Key Sulfur Oxidizing Bacteria." *Nature Communications* 9: 1–11. https://doi.org/10.1038/s41467-018-04041-x.

Canfield, D. E., F. J. Stewart, B. Thamdrup, et al. 2010. "A Cryptic Sulfur Cycle in Oxygen-Minimum-Zone Waters Off the Chilean Coast." *Science* 330: 1375–1378. https://doi.org/10.1126/science.1196889.

Christofi, N., T. Preston, and W. D. P. Stewart. 1981. "Endogenous Nitrate Production in an Experimental Enclosure During Summer Stratification." *Water Research* 15: 343–349. https://doi.org/10.1016/0043-1354(81)90039-7.

Cline, J. D. 1969. "Spectrophotometric Determination of Hydrogen Sulfide in Natural Waters." *Limnology and Oceanography* 14: 454–458. https://doi.org/10.4319/lo.1969.14.3.0454.

Cojean, A. N. Y., M. F. Lehmann, E. K. Robertson, B. Thamdrup, and J. Zopfi. 2020. "Controls of H_2S, Fe^{2+}, and Mn^{2+} on Microbial NO_3^--Reducing Processes in Sediments of an Eutrophic Lake." *Frontiers in Microbiology* 11: 1–17. https://doi.org/10.3389/fmicb.2020.01158.

Dong, L. F., M. N. Sobey, C. J. Smith, et al. 2011. "Dissimilatory Reduction of Nitrate to Ammonium, Not Denitrification or Anammox, Dominates Benthic Nitrate Reduction in Tropical Estuaries." *Limnology and Oceanography* 56: 279–291. https://doi.org/10.4319/lo.2011.56.1.0279.

Edgar, R. C. 2010. "Search and Clustering Orders of Magnitude Faster Than BLAST." *Bioinformatics* 26: 2460–2461. https://doi.org/10.1093/bioinformatics/btq461.

Edgar, R. C. 2013. "UPARSE: Highly Accurate OTU Sequences From Microbial Amplicon Reads" *Nature Methods* 10: 996-998. https://doi.org/10.1038/nmeth.2604.

Edgar, R. C. 2016. SINTAX: A Simple Non-Bayesian Taxonomy Classifier for 16S and ITS Sequences. bioRxiv. https://doi.org/10.1101/074161.

Ehrenfels, B., K. B. L. Baumann, R. Niederdorfer, et al. 2023. "Hydrodynamic Regimes Modulate Nitrogen Fixation and the Mode of Diazotrophy in Lake Tanganyika." *Nature Communications* 14: 1–13. https://doi.org/10.1038/s41467-023-42391-3.

Gardner, W. D. 1977. "Incomplete Extraction of Rapidly Settling Particles From Water Samplers." *Limnology and Oceanography* 22: 764–768. https://doi.org/10.4319/lo.1977.22.4.0764.

Gruber, N., and J. N. Galloway. 2008. "An Earth-System Perspective of the Global Nitrogen Cycle." *Nature* 451: 293–296. https://doi.org/10.1038/nature06592.

Hansen, H. P., and F. Koroleff. 1999. "Determination of Nutrients." In Methods of Seawater Analysis, edited by K. Grasshoff, K. Kremling, and M. Ehrhardt, 159–228. Wiley. https://doi.org/10.1002/9783527613984.ch10.

Holzner, C. P., W. Aeschbach-Hertig, M. Simona, M. Veronesi, D. M. Imboden, and R. Kipfer. 2009. "Exceptional Mixing Events in Meromictic Lake Lugano (Switzerland/Italy), Studied Using Environmental Tracers." *Limnology and Oceanography* 54: 1113–1124. https://doi.org/10.4319/lo.2009.54.4.1113.

Howarth, R. W., G. Billen, D. Swaney, et al. 1996. "Regional Nitrogen Budgets and Riverine N & P Fluxes for the Drainages to the North Atlantic Ocean: Natural and Human Influences." *Biogeochemistry* 35: 75–139. https://doi.org/10.1007/BF02179825.

Hulth, S., R. C. Aller, D. E. Canfield, et al. 2005. "Nitrogen Removal in Marine Environments: Recent Findings and Future Research Challenges." *Marine Chemistry* 94: 125–145. https://doi.org/10.1016/j.marchem.2004.07.013.

Kelso, B. H. L., R. V. Smith, R. J. Laughlin, and S. D. Lennox. 1997. "Dissimilatory Nitrate Reduction in Anaerobic Sediments Leading to River Nitrite Accumulation." *Applied and Environmental Microbiology* 63: 4679–4685. https://doi.org/10.1128/aem.63.12.4679-4685.1997.

Klotz, F., K. Kitzinger, D. K. Ngugi, et al. 2022. "Quantification of Archaea-Driven Freshwater Nitrification From Single Cell to Ecosystem Levels." *The ISME Journal* 16: 1647–1656. https://doi.org/10.1038/s41396-022-01216-9.

Könneke, M., A. E. Bernhard, J. R. de la Torre, C. B. Walker, J. B. Waterbury, and D. A. Stahl. 2005. "Isolation of an Autotrophic Ammonia-Oxidizing Marine Archaeon." *Nature* 437: 543–546. https://doi.org/10.1038/nature03911.

Lam, P., G. Lavik, M. M. Jensen, et al. 2009. "Revising the Nitrogen Cycle in the Peruvian Oxygen Minimum Zone." *Proceedings of the National Academy of Sciences* 106: 4752–4757. https://doi.org/10.1073/pnas.0812444106.

Lehmann, M. F., M. Simona, S. Wyss, et al. 2015. "Powering up the 'Biogeochemical Engine': The Impact of Exceptional Ventilation of a Deep Meromictic Lake on the Lacustrine Redox, Nutrient, and Methane Balances." *Frontiers in Earth Science* 3: 45. https://doi.org/10.3389/feart.2015.00045.

Lepori, F., M. Bartosiewicz, M. Simona, and M. Veronesi. 2018. "Effects of Winter Weather and Mixing Regime on the Restoration of a Deep Perialpine Lake (Lake Lugano, Switzerland and Italy)." *Hydrobiologia* 824: 229–242. https://doi.org/10.1007/s10750-018-3575-2.

Luo, J., X. Tan, K. Liu, and W. Lin. 2018. "Survey of Sulfur-Oxidizing Bacterial Community in the Pearl River Water Using soxB, sqr, and dsrA as Molecular Biomarkers." *3 Biotech* 8: 1–12. https://doi.org/10.1007/s13205-017-1077-y.

Naqvi, S. W. A., P. Lam, G. Narvenkar, et al. 2018. "Methane Stimulates Massive Nitrogen Loss from Freshwater Reservoirs in India." *Nature Communications* 9: 1–10. https://doi.org/10.1038/s41467-018-03607-z.

Ouyang, L., B. Thamdrup, and M. Trimmer. 2021. "Coupled Nitrification and N_2 Gas Production as a Cryptic Process in Oxic Riverbeds." *Nature Communications* 12: 1217. https://doi.org/10.1038/s41467-021-21400-3.

Pajares, S., M. M. Macek, and J. Alcocer. 2017. "Vertical and Seasonal Distribution of Picoplankton and Functional Nitrogen Genes in a High-Altitude Warm-Monomictic Tropical Lake." *Freshwater Biology* 62: 1180–1193. https://doi.org/10.1111/fwb.12935.

Pandey, C. B., U. Kumar, M. Kaviraj, K. J. Minick, A. K. Mishra, and J. S. Singh. 2020. "DNRA: A Short-Circuit in Biological N-Cycling to Conserve Nitrogen in Terrestrial Ecosystems." *Science of the Total Environment* 738: 139710. https://doi.org/10.1016/j.scitotenv.2020.139710.

Parada A. E., D. M. Needham, and J. A. Fuhrman. 2016. "Every Base Matters: Assessing Amall Subunit rRNA Primers for Marine Microbiomes with Mock Communities, Time Series and Global Field Samples." *Environmental Microbiology* 18: 1403–1414. https://doi.org/10.1111/1462-2920.13023.

Quast, C., E. Pruesse, P. Yilmaz, et al. 2013. "The SILVA Ribosomal RNA Gene Database Project: Improved Data Processing and Web-Based Tools." *Nucleic Acids Research* 41: 590–596. https://doi.org/10.1093/nar/gks1219.

Raghoebarsing, A. A., A. Pol, K. T. van de Pas-Schoonen, et al. 2006. "A Microbial Consortium Couples Anaerobic Methane Oxidation to Denitrification." *Nature* 440: 918–921. https://doi.org/10.1038/nature04617.

Risgaard-Petersen, N., S. Rysgaard, and N. P. Revsbech. 1995. "Combined Microdiffusion-Hypobromite Oxidation Method for Determining Nitrogen-15 Isotope in Ammonium." *Soil Science Society of America Journal* 59: 1077–1080. https://doi.org/10.2136/sssaj1995.03615995005900040018x.

Roland, F. A. E., F. Darchambeau, A. V. Borges, et al. 2018. "Denitrification, Anaerobic Ammonium Oxidation, and Dissimilatory Nitrate Reduction to Ammonium in an East African Great Lake (Lake Kivu)." *Limnology and Oceanography* 63: 687–701. https://doi.org/10.1002/lno.10660.

Schubert, C. J., E. Durisch-Kaiser, B. Wehrli, B. Thamdrup, P. Lam, and M. M. M. Kuypers. 2006. "Anaerobic Ammonium Oxidation in a Tropical Freshwater System (Lake Tanganyika)." *Environmental Microbiology* 8: 1857–1863. https://doi.org/10.1111/j.1462-2920.2006.001074.x.

Seitzinger, S. P. 1988. "Denitrification in Freshwater and Coastal Marine Ecosystems: Ecological and Geochemical Significance." *Limnology and Oceanography* 33: 702–724. https://doi.org/10.1057/9780230306912.

Shao, M. F., T. Zhang, and H. H. P. Fang. 2010. "Sulfur-Driven Autotrophic Denitrification: Diversity, Biochemistry, and Engineering Applications." *Applied Microbiology and Biotechnology* 88: 1027–1042. https://doi.org/10.1007/s00253-010-2847-1.

Shapleigh, J. P. 2013. "Denitrifying Prokaryotes." In The Prokaryotes—Prokaryotic Physiology and Biochemistry, edited by E. Rosenberg, E. F. DeLong, S. Lory, E.

Stackebrandt, and F. Thompson, 405–425. Springer-Verlag Berlin Heidelberg.

Strohm, T. O., B. Griffin, W. G. Zumft, and B. Schink. 2007. "Growth Yields in Bacterial Denitrification and Nitrate Ammonification." *Applied and Environmental Microbiology* 73: 1420–1424. https://doi.org/10.1128/AEM.02508-06.

Studer, A. S., L. Wörmer, H. Vogel, et al. 2024. "First Lacustrine Application of the Diatom-Bound Nitrogen Isotope Paleo-Proxy Reveals Coupling of Denitrification and N_2 Fixation in a Hyper-Eutrophic Lake." *Limnology and Oceanography* 69: 1797–1809. https://doi.org/10.1002/lno.12627.

Su, G., M. F. Lehmann, J. Tischer, et al. 2023. "Water Column Dynamics Control Nitrite-Dependent Anaerobic Methane Oxidation by *Candidatus* 'Methylomirabilis' in Stratified Lake Basins." The *ISME Journal* 17: 693–702. https://doi.org/10.1038/s41396-023-01382-4.

Suter, E. A., M. I. Scranton, S. Chow, D. Stinton, L. Medina Faull, and G. T. Taylor. 2017. "Niskin Bottle Sample Collection Aliases Microbial Community Composition and Biogeochemical Interpretation." *Limnology and Oceanography* 62: 606–617. https://doi.org/10.1002/lno.10447.

Thamdrup, B., and T. Dalsgaard. 2002. "Production of N_2 Through Anaerobic Ammonium Oxidation Coupled to Nitrate Reduction in Marine Sediments." *Applied and Environmental Microbiology* 68: 1312–1318. https://doi.org/10.1128/AEM.68.3.1312.

Thamdrup, B., T. Dalsgaard, M. M. Jensen, O. Ulloa, L. Farias, and R. Escribano. 2006. "Anaerobic Ammonium Oxidation in the Oxygen-Deficient Waters Off Northern Chile." *Limnology and Oceanography* 51: 2145–2156. https://doi.org/10.4319/lo.2006.51.5.2145.

Tischer, J., J. Zopfi, C. Frey, et al. 2025. "Nitrogen and Oxygen Isotope Effects during Enzymatic Nitrate Reduction In Vitro and by Natural Lake Water Consortia." *bioRxiv*. https://doi.org/10.1101/2025.03.29.645582.

Wenk, C. B., J. Blees, J. Zopfi, et al. 2013. "Anaerobic Ammonium Oxidation (Anammox) Bacteria and Sulfide-Dependent Denitrifiers Coexist in the Water Column of a Meromictic South-Alpine Lake." *Limnology and Oceanography* 58: 1–12. https://doi.org/10.4319/lo.2013.58.1.0001.

Wenk, C. B., J. Zopfi, J. Blees, M. Veronesi, H. Niemann, and M. F. Lehmann. 2014. "Community N and O Isotope Fractionation by Sulfide-Dependent Denitrification and Anammox in a Stratified Lacustrine Water Column." *Geochimica et Cosmochimica Acta* 125: 551–563. https://doi.org/10.1016/j.gca.2013.10.034.

Yao, X., J. Wang, M. He, et al. 2024. "Methane-Dependent Complete Denitrification by a Single *Methylomirabilis* Bacterium." *Nature Microbiology* 9: 464–476. https://doi.org/10.1038/s41564-023-01578-6.

Zopfi, J., M. E. Böttcher, and B. B. Jørgensen. 2008. "Biogeochemistry of Sulfur and Iron in *Thioploca*-Colonized Surface Sediments in the Upwelling Area off Central Chile." *Geochimica et Cosmochimica Acta* 72: 827–843. https://doi.org/10.1016/j.gca.2007.11.031.

Zumft, W. G. 1997. "Cell Biology and Molecular Basis of Denitrification." *Microbiological and Molecular Biology Reviews* 61: 533–616. https://doi.org/10.1128/.61.4.533-616.1997.

Supporting Information

Additional Supporting Information may be found in the online version of this article.

Submitted 09 December 2024
Revised 04 July 2025
Accepted 30 December 2025